IEEE/CSC & ESAS European Superconductivity News Forum (ESNF), No. 6, October 2008
(ASC Preprint 3EC04 conforming to IEEE Policy on Electronic Dissemination, Section 8.1.9)

This manuscript should be cited as IEEE Transactions on Applied Superconductivity, submitted 2008.

Quantum Efficiency and Polarization Effects in NbN Superconducting Single Photon Detectors

Laurent Maingault, Paul Cavalier, Roch Espiau de Lamaëstre, Laurent Frey, and Jean-Claude Villégier

***Abstract*—Superconducting Single Photon Detectors based on niobium nitride (NbN) nanowires have been optimized in regards to the quality of the epitaxial layer grown on M-plane 3-inch Sapphire wafer, leading to $T_c \approx 13\,\mathrm{K}$ and $J_c \approx 5\,\mathrm{MA/cm^2}$ for a $5\,\mathrm{nm}$ thick layer patterned down to $80\,\mathrm{nm}$ stripe width using an e-beam writer. Using those films, 7 % of quantum efficiency at $4.2\,\mathrm{K}$ for $100\,\mathrm{nm}$ linewidth nanowires detectors has been achieved. We measured the kinetic inductance of our SSPD by 2 differents ways. Clear effects of light polarization on Detection Efficiency (DE) dependent has also been observed and quantified. DE varies by a factor 2 to 4 for a great number of tested SSPDs, meander width varying from $100\,\mathrm{nm}$ to $300\,\mathrm{nm}$. The SSPD has been modeled as a detector with 2 different linear DEs as incident light can be polarized parallel or normal to the linewidth. This model is in good agreement with experimental data and roughly corresponds to the calculated absorption of the $5\,\mathrm{nm}$ thick NbN layer. However polarization effects also observed in multi-photon regime raise new issues.**

***Index Terms*—NbN, superconducting single photon detector, thin films, light polarization, quantum optics, FDTD simulation**

I. Introduction

SSPD offers great opportunity to single photon detection [1]. Very high Detection Efficiencies (DE) have already been realized [2] as well as the photon-counting ability [3]. This type of detector should bring major achievements in quantum optics [4] and applications in astronomy [5], especially in near infrared wavelengths. However, DE, which corresponds to the whole system efficiency, is still below semiconductor's state-of-art detectors, such as Avalanche PhotoDiode, justifying ongoing efforts to enhance it by improving the coupling of the incoming signal to the detector, the absorption probability of photons by a very thin NbN nanowire and the quality and geometry of the latter nanowire. Attention was however lower with respect to other drawbacks of those detectors such as polarization effects. For example, it has been recently pointed out that the DE is rather different whether the incoming light polarization is perpendicular or parallel to the nanowire axis [6], which could be detrimental for some applications. Noteworthingly, the authors' explanation for this assertion involves some internal efficiency of hot spot generation after the optical absorption event took place. In this article, we tackle this issue of polarization dependence by investigating it in the multi-photon detection regime, and stress the importance of a careful determination of the optical index of NbN ultrathin films into the determination of the polarization ratio of DE. This study was made possible by the development of an electro-optical characterization set-up that is also detailed.

Manuscript received August 23, 2008.
This work was supported in part by the contract EC "Sinphonia" NMP4-CT-2005-16433.

L. Maingault, P. Cavalier and J-C. Villégier are with the Institute of Nanosciences and Cryogenics (INAC) SPSMS CEA-Grenoble, 38054 GRENOBLE-Cedex-9, France
R.Espiau de Lamaëstre, L. Frey are with CEA/LETI MINATEC, 38054 GRENOBLE-Cedex-9, France
Corresponding author is Laurent Maingault, phone: 33+438786023; fax: 33+438785096; e-mail: laurent.maingault@cea.fr

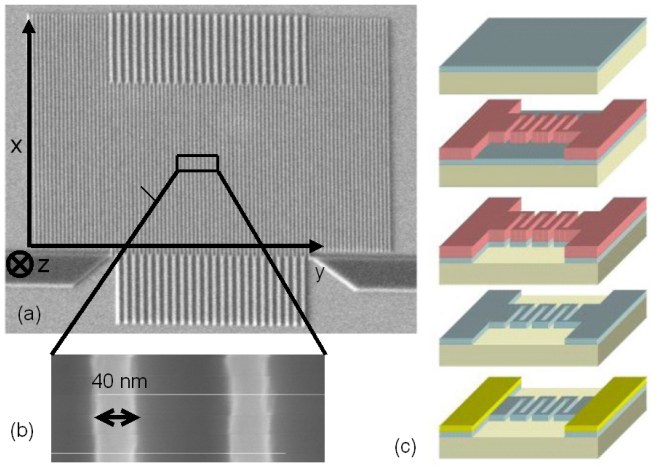

Fig. 1. (a) SEM top-picture of a $3\,\mu\mathrm{m}\times3\,\mu\mathrm{m}$ SSPD. (b) A zoom shows a 40 nm linewidth (c) Schematic of the processing steps. From top to bottom: NbN growth, e-beam lithography, NbN etching, resist stripping, contact (Ti/Au) deposition.

II. Experiment

A. Fabrication

Superconductive ultrathin NbN films are DC-magnetron sputtered using a Ar/N_2 plasma and typically have a critical supercurrent of $5.5\,\mathrm{MA/cm^2}$ and critical temperature of about $13\,\mathrm{K}$ for a 5 nm thick film. More details about thin film growth and characterization are given in Ref. [7]. The best transport properties are obtained after untwinned growth on M-plane sapphire substrate [8]. A 100-kV e-beam writer then allows patterning of SSPD's NbN nanowire, using Sumitomo NEB-22A2 negative resist, forming typical meander shape that can be observed by SEM in Fig. 1 (a) and (b). The following process is shown on Fig. 1 (c) and developed in Ref. [9].

With this process, SSPDs with 7% DE were achived with a 90 nm linewidth and $3\,\mu\mathrm{m} \times 3\,\mu\mathrm{m}$. This is not too far from the state-of-the-art raw detectors because the measurements were done at 4.2K with a $1.55\,\mu\mathrm{m}$ light wavelength.

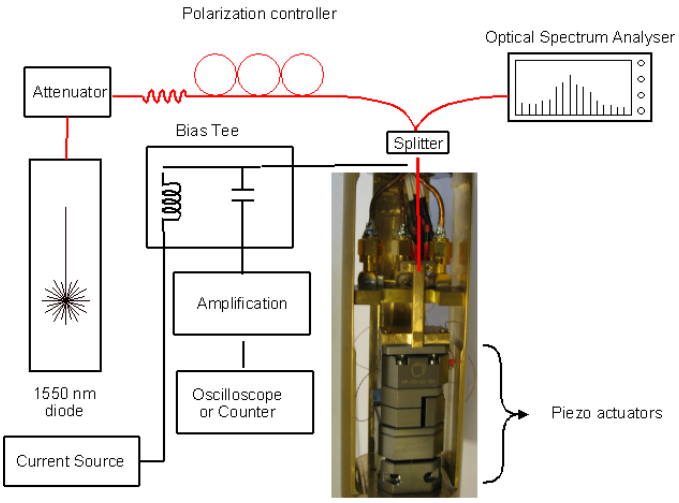

Fig. 2. Schematic of our electro-optical set-up, operating at telecom wavelength (1550 nm)

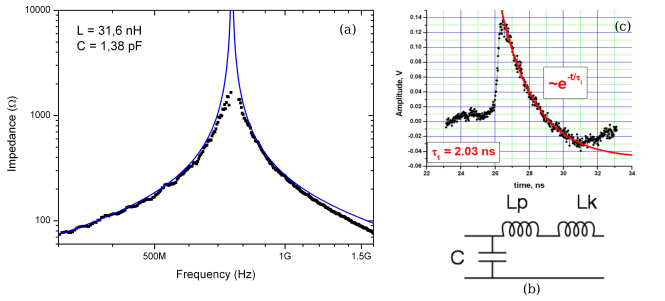

Fig. 3. Kinetic inductance measurements of SSPDs. (a) Vector Network Analyzer (VNA) spectrum of a 500 nm-wide nanowires SSPD. The peak corresponds to the L–C resonance at frequency $F = \sqrt{LC}$. (b) Schematic of the model circuit in order to fit VNA spectrum. (c) Typical pulse response of a SSPD. The decay time is proportional to $L/50\,\Omega$.

B. Characterization

Samples are tested in liquid He (4.2 K). They are DC current-polarized using low current noise batteries trough a bias-tee as shown in Fig. 2. A photon absorption by the NbN film can create a resistive state, a so-called "hot-spot". This produces a short pulse which is amplified (40 dB /20 GHz) before being monitored either on an 3 GHz single-shot oscilloscope or statistically analyzed with the help of a photon counter (Stanford Research SR400).

1) Kinetic inductance measurements: A Hewlett Packard 100 MHz–20 GHz Vectorial Network Analyzer (VNA) determines our circuit impedance, and so on the nanowires' impedance as described later. SSPD's response time is most probably limited by kinetic inductance [10]. The decay time is proportional to $\exp(-L/R)$, where L is the wire kinetic inductance $R = 50\,\Omega$ is the RF cable impedance. Fig. 3 (a) shows a typical spectrum from the VNA, at sufficient low power (45 dBm) to keep the superconducting regime. Considering that a SSPD is part of a L–C circuit, with capacitance C including all the parasitic capacities induced at high frequency. We can fit this spectrum by the theoretical curve for this first-order filter and then determine the nanowire's kinetic inductance. Within the fitting procedure, we took into account the parasitic bonding inductances (L_p). With all this procedure we were able to calculate the $L_\square$ of our films. NbN growth on R-plane sapphire gives a higher value as compared to M-plane.

2) Optical set-up: Samples are illuminated by a superluminescent diode at a wavelength around $\lambda = 1550\,\text{nm}$, whose spectrum is about 100 nm large. All the light is guided with single-mode optical fibers (normal or polarization-maintaining) through the SSPD. The very low input power needed to obtain single photon regime are obtained with an HP variable attenuator. Efficiently coupling light to the SSPD [11] is a major issue to improve DE and needs to be addressed for applications. In our case, this is achieved thanks to piezoelectric actuators that accurately controls the fiber position in 3 dimensions. This allows us to fine tune the alignment of the fiber with respect to the SSPD. However, one needs to know where the fiber is. First, we used the spectral properties of the reflected laser excitation in order to determine the distance d between the fiber and the detector in the z direction. This distance, d, is then directly given by the inter fringe, $\Delta\lambda$ ($d = \Delta\lambda/2\lambda^2$), with an uncertainty below 1%. Fig 4 (a) shows a SSPD DE as a function of the distance d. As expected, DE increases when d decreases.

Moreover, the light going out is quite accurately modeled by a gaussian waveform with its waist (5 μm for a 1550 nm single mode fiber) at the end of the fiber. Taking into account the SSPD size, the expected dependence of DE versus d and ρ (lines on Fig 4 (a) and (b)) is calculated, thus proving that all the expected light actually hits the SSPD. In the ρ direction (normal to the fiber), the center of the light waveform is obviously at the position where counts rate is at its maximum. Then position is directly calculated knowing this maximum count rate and d.

In order to control the light polarization incoming on the SSPD, we inserted a polarization controller. It classically consists of a polarizer, a quarter-wave and a half-wave plates. Each of these elements can have any angle with respect to the others, thus generating any possible polarization state from the diode unpolarized light. Note that the fiber in-between the polarization controller and the sample may be birefringent, but it is kept constant during one measurement. With this optical set-up, polarization effects for our SSPDs are characterized with reproducible results thanks to our highly controlled of fiber position.

III. Polarization Effects

A. Polarization dependency and simulation

We found out that SSPD's DE is strongly light polarization dependent, as already stated in [6]. This dependency can be characterized by R, ratio of highest DE for a given polarization to the lowest. Detectors with lines between 90 and 300 nm and filling factor around 50% were polarization characterized. R was measured between 2 and 4 at 4.2 K, with no clear dependency on the aforementioned parameters. Though, a dependence on the fiber position was observed: R decreases when fiber is far (more than 1 μm), probably due to light unpolarized reflections incoming on the SSPD.

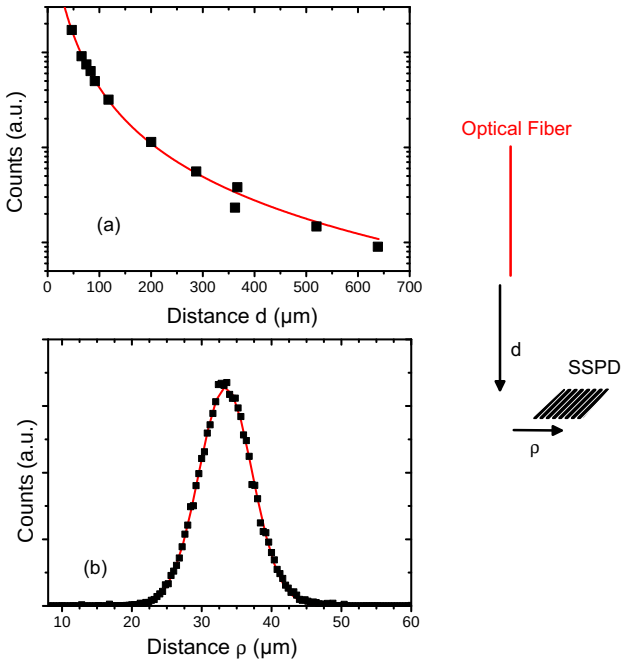

Fig. 4. (a) Detection Efficiency (DE) with respect to the distance of the fiber. This scales well with a gaussian model (line). (b) DE with respect to distance ρ, taken at $d = 400\,\mu$m. This fits well with gaussian waist of $40\,\mu$m, expected at this distance (line).

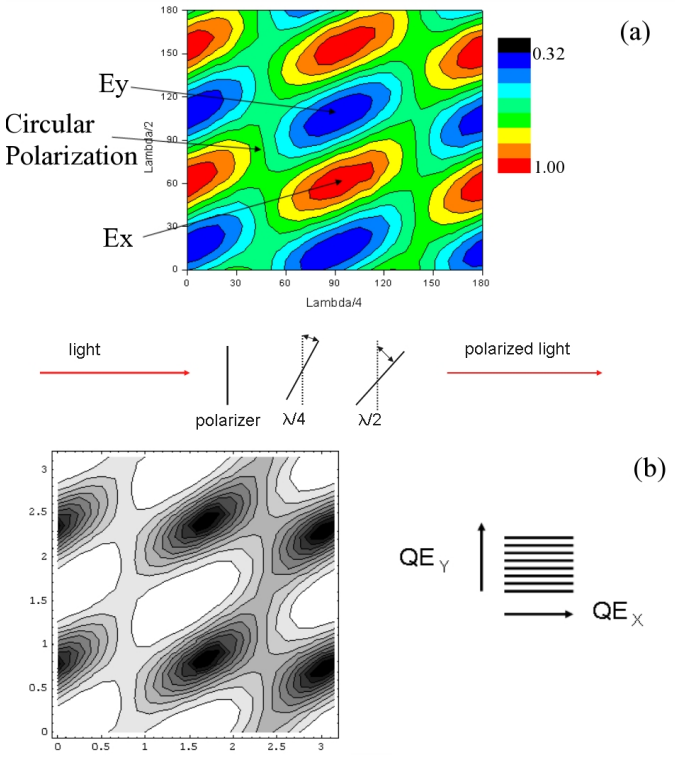

Fig. 5. (a) Detection Efficiency for a typical SSPD (100 nm linewidth, 50% filling factor) with respect to wave-plate angles of the polarization controller. Remarkable zones are pointed on the contour plot. (b) Simulation of this polarization dependence when considering that DE is different from an electric field along the x or y axis

More surprisingly, R decreases when ρ increases, which is not understood.

Figure 5 shows a typical graph of DE dependency with respect to wave-plate angles. Zones with high DE correspond to a linear polarization, parallel to the meander lines (x direction in Fig. 1), as discussed later. On the opposite, the lowest DE is observed when electric field is orthogonal to the meander lines, that is for the half-wave plate rotated by 45° from the previous described position. This exactly corresponds to what we obtain on Fig. 5.

Moreover, we can simulate this effect by considering 2 different DE for each polarization: DE_x and DE_y. Experimental data are well reproduced by adjusting the last optical fiber birefringence, which is usually quite low if the fiber is not twisted (dephasing below $\Pi/12$). This effect can be understood if we consider that absorption of NbN is very different for an electric field parallel or perpendicular to the nanowires. To explain this DE difference, Finite Difference Time Domain calculations were performed and proved that absorption is more efficient when electric field is parallel to the wires. Quantitatively, simulations give an absorption of 21% for polarized light along x compared to 10% along y for a 100 nm SSPD and filling factor of 50%. However, the uncertainty of NbN ultrathin film optical index makes it hard to clearly quantify this difference.

B. Polarization in multi-photon regime

If we current-bias SSPD in multiphoton regime, say N-photon regime, we observe an increasing ratio, R_N. Quite impressively, one can almost switch off the DE in the y polarization, when N is high enough. For instance, Fig. 6 (b) shows a totally extincted signal for y polarization in a regime with many photons. This is almost a polarization detector even though this regime is quite unstable and rapidly saturates as observed in the center of x polarization.

Fig. 6 shows the ratio dependence with decreasing bias current. The ratio is increased for decreased currents simply because the photon regime is increased. However, if we estimate the number of photons by the traditional mean [12] (see Fig. 6 (a)), the experimental ratio is not as high as expected.

IV. Conclusion

As a conclusion, we showed our capability to fabricate and characterize SSPDs on R-plane or more interesting M-plane sapphire substrates. The whole process finally gives DE of 7% at 4.2 K (on R-plane). The whole electro-optical set-up allows to measure SSPD's kinetic inductances and optical properties. High light polarization dependence of SSPD were demonstrated. This effect is most probably due to different absorption of incoming light polarization of the NbN films, as checked by numerical calculations. This effect needs to be taken into account for further applications, where the incoming light usually have an unknown polarization. Further integration of SSPD with other devices [5] or enhancement of NbN optical absorption will be adressed, taking into account this polarization issue.

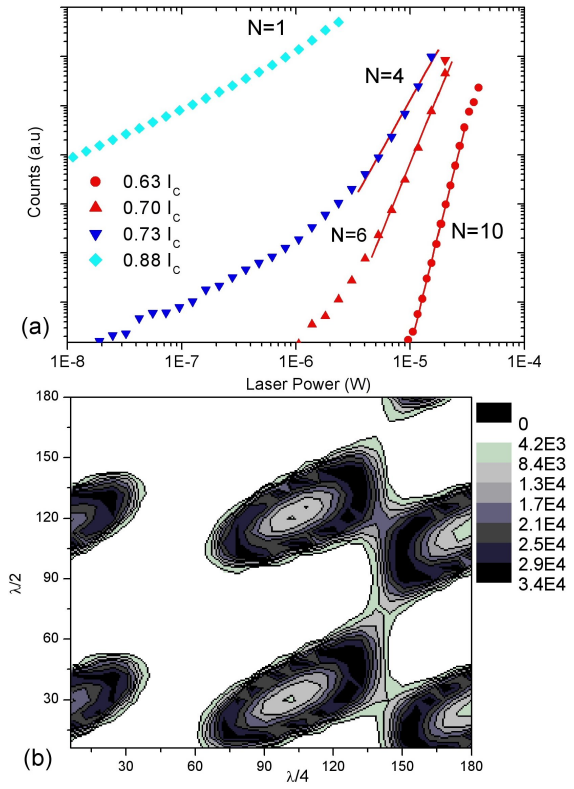

Fig. 6. (a) Photon regime determined by plotting the count rate vs incoming laser power. The slope of the graph indicates the regime, which depends on laser power *and* current polarization. This figure is obtained with a 200-nm and 50% filling factor SSPD. (b) Photon regime determined by polarization dependence. Here the ratio R is enhanced because of multi-photon regime.

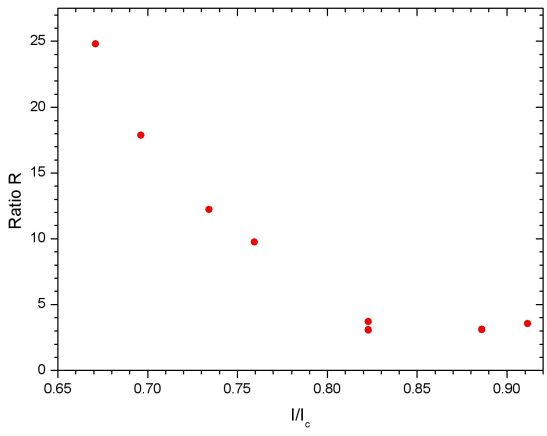

Fig. 7. Experimental polarization ratio, R, dependent on the DC bias current. For low bias current, R is enhanced due to multi-photon counting regime.

ACKNOWLEDGMENT

The authors would like to thank C. Constancias (CEA-LETI), J.-L. Thomassin (CEA-INAC) for performing the e-beam lithography, the "Plateforme de Technologie Amont" (PTA) for fabrication equipment and its support.

REFERENCES

[1] G. N. Gol'tsman, O. Okunev, G. Chulkova, A. Lipatov, A. Semenov, K. Smirnov, B. Voronov, A. Dzardanov, C. Williams, and R. Sobolewski, "Picosecond superconducting single-photon optical detector," *Applied Physics Letters*, vol. 79, no. 6, pp. 705–707, 2001. [Online]. Available: http://link.aip.org/link/?APL/79/705/1

[2] K. M. Rosfjord, J. K. W. Yang, E. A. Dauler, A. J. Kerman, V. Anant, B. M. Voronov, G. N. Gol'tsman, and K. K. Berggren, "Nanowire single-photon detector with an integrated optical cavity and anti-reflection coating," *Opt. Express*, vol. 14, no. 2, pp. 527–534, 2006. [Online]. Available: http://www.opticsexpress.org/abstract.cfm?URI=oe-14-2-527

[3] A. Divochiy, F. Marsili, D. Bitauld, A. Gaggero, R. Leoni, F. Mattioli, A. Korneev, V. Seleznev, N. Kaurova, O. Minaeva, G. Gol'tsman, K. G. Lagoudakis, M. Benkhaoul, F. Levy, and A. Fiore, "Superconducting nanowire photon-number-resolving detector at telecommunication wavelengths," *Nature Photonics*, vol. 2, no. 5, pp. 302–306, May 2008. [Online]. Available: http://dx.doi.org/10.1038/nphoton.2008.51

[4] H. Takesue, S. W. Nam, Q. Zhang, R. H. Hadfield, T. Honjo, K. Tamaki, and Y. Yamamoto, "Quantum key distribution over a 40-db channel loss using superconducting single-photon detectors," *Nat Photon*, vol. 1, no. 6, pp. 343–348, Jun. 2007. [Online]. Available: http://dx.doi.org/10.1038/nphoton.2007.75

[5] E. le Coarer, S. Blaize, P. Benech, I. Stefanon, A. Morand, G. Lerondel, G. Leblond, P. Kern, J. M. Fedeli, and P. Royer, "Wavelength-scale stationary-wave integrated fourier-transform spectrometry," *Nature Photonics*, vol. 1, no. 8, pp. 473–478, Aug. 2007. [Online]. Available: http://dx.doi.org/10.1038/nphoton.2007.138

[6] V. Anant, A. J. Kerman, E. A. Dauler, J. K. W. Yang, K. M. Rosfjord, and K. K. Berggren, "Optical properties of superconducting nanowire single-photon detectors," *Opt. Express*, vol. 16, no. 14, pp. 10 750–10 761, 2008. [Online]. Available: http://www.opticsexpress.org/abstract.cfm?URI=oe-16-14-10750

[7] J.-C. Villégier, N. Hadacek, S. Monso, B. Delaët, A. Roussy, P. Febvre, G. Lamura, and J.-Y. Laval, "Nbn multilayer technology on r-plane sapphire," *Applied Superconductivity, IEEE Transactions on*, vol. 11, no. 1, pp. 68–71, Mar 2001.

[8] R. E. de Lamaëstre, P. Odier, and J.-C. Villégier, "Microstructure of nbn epitaxial ultrathin films grown on a-, m-, and r-plane sapphire," *Applied Physics Letters*, vol. 91, no. 23, p. 232501, 2007. [Online]. Available: http://link.aip.org/link/?APL/91/232501/1

[9] C. Constancias, R. E. de Lamaëstre, O. Louveau, P. Cavalier, and J.-C. Villégier, "Patterning issues in superconducting nanowire single photon detector fabrication," vol. 25, no. 6. AVS, 2007, pp. 2041–2044. [Online]. Available: http://link.aip.org/link/?JVB/25/2041/1

[10] A. J. Kerman, E. A. Dauler, W. E. Keicher, J. K. W. Yang, K. K. Berggren, G. Gol'tsman, and B. Voronov, "Kinetic-inductance-limited reset time of superconducting nanowire photon counters," *Applied Physics Letters*, vol. 88, no. 11, p. 111116, 2006. [Online]. Available: http://link.aip.org/link/?APL/88/111116/1

[11] W. Slysz, M. Wegrzecki, J. Bar, P. Grabiec, M. Górska, V. Zwiller, C. Latta, P. Bohi, I. Milostnaya, O. Minaeva, A. Antipov, O. Okunev, A. Korneev, K. Smirnov, B. Voronov, N. Kaurova, G. Gol'tsman, A. Pearlman, A. Cross, I. Komissarov, A. Verevkin, and R. Sobolewski, "Fiber-coupled single-photon detectors based on nbn superconducting nanostructures for practical quantum cryptography and photon-correlation studies," *Applied Physics Letters*, vol. 88, no. 26, p. 261113, 2006. [Online]. Available: http://link.aip.org/link/?APL/88/261113/1

[12] R. Sobolewski, A. Verevkin, G. Gol'tsman, A. Lipatov, and K. Wilsher, "Ultrafast superconducting single-photon optical detectors and their applications," *Applied Superconductivity, IEEE Transactions on*, vol. 13, no. 2, pp. 1151–1157, June 2003.